

Drone survey provides preliminary insights into the biological aspects of Bryde's whales in southeastern Brazil

Lucas Lima de Oliveira¹, Ticiana Fettermann², Renata Karina Marconi Marcançoli³,
and Daniel Danilewicz^{2,3}

¹Instituto Aqualie, Juiz de Fora, Brazil

²Grupo de Estudos de Mamíferos Aquáticos do Rio Grande do Sul (GEMARS), Torres, Brazil

³Programa de Pós-graduação em Zoologia, Universidade Estadual de Santa Cruz (UESC), Ilhéus, Brazil

*Corresponding author: llimaoliveira@hotmail.com

Bryde's whales (*Balaenoptera edeni*) are distributed worldwide in tropical and temperate waters and are considered one of the least known Balaenopteridae species (Kato & Perrin, 2018). The species is classified as Least Concern by the IUCN Red List (Thomas et al., 2016) and Data deficient by the Red Book of Endangered Brazilian Fauna (ICMBio, 2018). Its taxonomy is unresolved and genetic studies have proposed the existence of two provisional subspecies, *Balaenoptera edeni edeni* and *B. e. brydei*, the latter occurring in Brazilian waters (Pastene et al., 2015; Kato & Perrin, 2018).

Bryde's whales occur in both shallow and deep waters, and their latitudinal shifts are mainly related to variations in the distribution of food resources (Lodi et al., 2015; Kato & Perrin, 2018). The species has been reported in different regions of Brazil and is regularly observed in the southern and southeastern areas (Maciel et al., 2018; Lima, 2020; Milmann et al., 2020). The highest sighting rates occur during the austral spring and

summer months when they are typically seen alone or in small groups of 2 – 3 individuals. It has been suggested that Bryde's whales are resident in Brazilian waters throughout the year (Athayde et al., 2020), not showing large migratory movements (Chivers, 2009; Lodi et al., 2015; Lodi & Tardin, 2018), and the variability of sightings are likely to be associated to the presence, abundance, and distribution of food sources (Maciel et al., 2018; Athayde et al., 2020).

High-resolution aerial drone imagery can allow detailed observations and be very informative, providing data on respiratory cycles, travel speed, morphometric measurements, body condition, individual marks, behavior, and group composition for numerous cetacean species (Baxter & Hamilton, 2018; Burnett et al., 2019; Fettermann et al., 2022; de Oliveira et al., 2023). Here, we present a case study applying high-resolution drone monitoring of Bryde's whales based on an opportunistic sighting in Ubatuba, southeastern Brazil.

On 14 December 2021, a solitary Bryde's whale was sighted traveling slowly in coastal waters (ca. 16 m deep) at Ubatuba (23° 25' 58" S, 45° 04' 15" W) (Fig. 1). The opportunistic encounter occurred aboard a 4.7 m aluminum vessel during a survey for Franciscana dolphins (*Pontoporia blainvillei*). The whale was first sighted at 9:10 am and ended at 9:45 am. The boat approached the whale following the good practices for the sighting of marine mammals and Instituto Brasileiro do Meio Ambiente e dos Recursos Naturais Renováveis (IBAMA) ordinance nº 117, reducing the speed and moving at idle speed at a minimum distance of 100 m to minimize behavioral impacts (IBAMA, 2002; Júnior et al., 2019).

The initial observation assessed animal behavior and environmental conditions (Beaufort 1 and wind gusts < 10 knots). After that, two consecutive flights were performed to collect focal individual follow data using a DJI Phantom 4 (camera 1" CMOS Sensor, FOV 8.8 mm, and sensor size 13.2 x 8.8 mm). The drone took off and landed in the hand of an assistant at an altitude of 2.1 m above sea level. During the flight, a high-resolution image was recorded (4K - 3840 x 2160 pixels, pixel dimension

Keywords:

Balaenoptera edeni, morphometric, conservation, photogrammetry, aerial imagery

ARTICLE INFO

Manuscript type: Note

Article History

Received: 14 March 2023

Received in revised form: 26 June 2023

Accepted: 03 July 2023

Available online: 27 October 2023

Handling Editor: Nataly Castelblanco-Martinez

Citation:

de Oliveira, L. L., Fettermann, T., Marcançoli, R. K. M., & Danilewicz, D. (2023). Drone survey provides preliminary insights into the biological aspects of Bryde's whales in southeastern Brazil. *Latin American Journal of Aquatic Mammals*, 18(2), 224-230. <https://doi.org/10.5597/lajam00314>

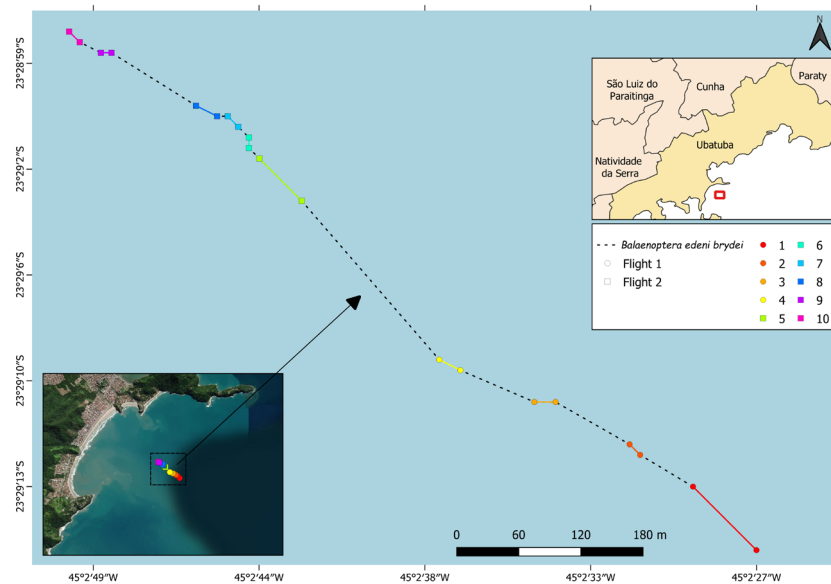


Figure 1. Map illustrating the location and drone monitoring track conducted during the Bryde's whale encounter. The color points indicate the respiratory cycles monitored in flights 1 (circles) and 2 (squares).

= 0.0034 mm/pixel) with 90° gimbal pitch down, and the whale always centered in the field of view of the camera to avoid the lens distortion effect (Dawson et al., 2018; Burnett et al., 2019), and altitude between 20 to 30 m above sea level to minimize potential interference in the animal's behavior (Fettermann et al., 2019; Fearnbach et al., 2020). Approximately six minutes of individual focal follow were collected during the two flights (3.13 and 3.08 minutes for flights 1 and 2, respectively).

Each video was visually processed to extract information about the respiratory cycles. Here, the respiratory cycle was defined as the inter-breath interval (in seconds), i.e., the period between the last breath before diving and being submerged until returning from the dive to breathe again. Submerged time was defined as the time spent underwater between respiratory cycles, visibility time when the whale was at the surface and visible to the boat-based observer, and availability time was defined as the time that the whale was visible by the drone. Due to water transparency (estimated as 1.5 - 2 m), availability time may be higher than visibility time. Based on this classification, the number of respiratory cycles, the submerged time, availability, and visibility time were estimated in seconds.

To estimate the swimming speed of the Bryde's whale, the total distance traveled (in meters) was divided by the difference between the time of the first moment of breathing (flight 1) and the time of the last (flight 2). For this, the proxy distances traveled between each respiratory cycle were calculated from the latitude and longitude obtained by the drone GPS metadata for each cycle. This was possible as the drone was maintained directly above the focal individual during the focal follow. The interval between the two flights (in seconds) and the distance performed during this time were added to the total time, and distance traveled in the analyses. This was feasible looking at the last GPS location from flight 1 to the first GPS location on flight 2.

For aerial photogrammetry analyses, each video was visually processed (viewed using VLC Media Player software, version

3.0.17.4) to extract full-resolution still images of the whale at the surface using the snapshot function. Four frames of adequate quality were obtained at altitudes of 21 m (n = 2) and 31 m (n = 2). Frames were selected to meet standard criteria for photogrammetry, such as clear focus, elongated body at the surface, the tip of the rostrum, caudal notch, and the body contour visible, and no body-arching and the whale centered in the field of view of the camera (Christiansen et al., 2016; Durban et al., 2016; de Oliveira et al., 2023), these steps were adopted to avoid possible inaccuracies during the analysis, such as lens distortion or body curvature, which could overestimate or underestimate the collected measurements.

Morphometric measurements were obtained using an aerial photogrammetry protocol like those described by de Oliveira

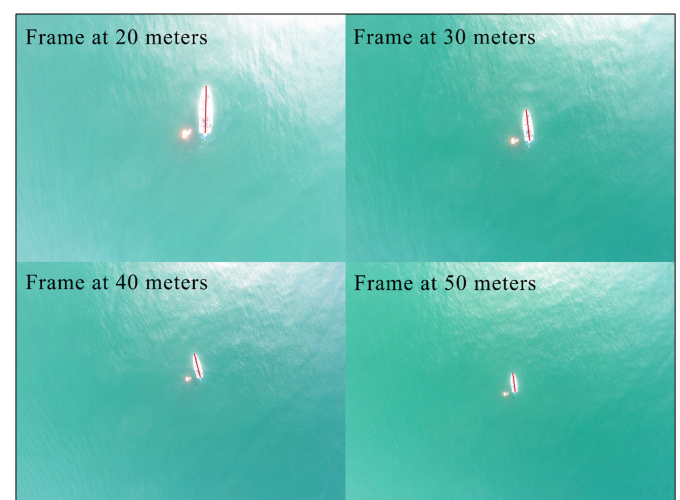


Figure 2. Frames used to generate the calibration model considering the measurements of the boat at different altitudes. The red lines represent the pixel measurement collected from the 4.7-m-long boat at each flight altitude.

et al. (2023) and Ratsimbazafindranahaka et al. (2022). This method involved measuring a scale object at different altitudes to calibrate the pixel measurements and convert them to scalar measurements using the empirical Ground Sample Distance (eGSD). Before the whale sighting, a 4.7-meter-long boat was imaged three times at 20, 30, 40, and 50 meters to estimate the eGSD.

Accurately determining flight altitude poses a significant challenge in aerial photogrammetry analysis, mainly due to inconsistencies in the barometric sensors of commercial drones (Bierlich et al., 2021). Thus, in Burnett et al. (2019), Ratsimbazafindranahaka et al. (2022), and Oliveira et al. (2023) the frames used for whale measurements did not include a framed scale object. As a result, it is not feasible to directly assess the associated error in determining the flight altitude presented by the barometric sensor. To mitigate this potential error, a regression model was proposed to establish a relationship between expected (Exp Altitude) and observed flight altitudes (Ratsimbazafindranahaka et al., 2022). The Exp Altitude was calculated using the equation (1):

$$Exp\ Altitude = \frac{eGSD \cdot Pixel\ dimension}{Focal\ Length}$$

Here, eGSD was calculated as the object length (m) divided by the object length in pixels. The pixel dimension for the image was 0.0034 mm/pixel, and the focal length was 8.8 mm. This approach estimates the altitude at which the drone would need to be positioned to provide the eGSD. The Exp Altitude was then regressed against the barometer altitude, yielding the coefficients used to estimate the Exp Altitude for the whale frames. The frames were measured using ImageJ software ver. 1.53k, and the models were constructed in R ver. 4.2.3 using the *lm* function. Once we have a model fitted and validated, we can get the correct GSD used to estimate the whale's measurements.

For each Bryde's whale frame, 11 measurements attributes (in pixels) were obtained: the total body length (BL) (distance from

the tip of the rostrum to the notch of the fluke), the body width at 10% intervals along the body length (10% - 90% BL) and the fluke width (FW).

The standardized whale measurements were the mean of the estimated measurements in all four frames. Data were tested for normality and variance equality using the Shapiro-Wilk and Levene's tests. All tests and statistical analyses were performed in R (version 4.2.3). To identify possible mean differences in the measurement estimates at each flight altitude (21 and 31 m), a two-sample Fisher-Pitman Permutation Test was applied using the *oneway_test* function from the coin package with Bonferroni *p-value* correction.

Ten complete respiratory cycles were recorded and analyzed during the 373 seconds of focal follow video recording (flight 1, *n* = 4; flight 2, *n* = 6; Fig. 3). Submersion and availability time data did not show normality. The median submerged and availability time were 20.5 s and 27.0 s, respectively, while the median visibility time was 6.5 s (SD = 1.2 s). Only one breath was recorded between each submersion, regardless of its duration. Throughout the observation (373 s), the whale remained submerged for 309 s (83% of the time), although it was available to the drone's field of view for 373 s (100% of the time), only visible to the boat observer for 64 s (17%). Thus, drone recording increased the observation capacity fivefold.

Considering the bathymetry of the collection area (maximum depth of 8 - 10 meters) and the availability time data (100% of the video time), during the time of image collection the whale presented only shallow dives, not exceeding 3 m deep. During shallow dives, Dong et al. (2022) estimated the submerged time of Bryde's whales in Shenzhen, China, using satellite suction transmitters, at about 18.36 ± 13.30 seconds in contrast to the 30.9 ± 22.56 seconds observed in this work. These differences may be associated with the spatial resolution of the analyses, as telemetry data may provide more localization points to estimate the dive parameters in a wide range compared to the small fraction of time obtained in the present study.

The whale was observed to travel a total distance of 883 meters in 514.20 s (8.57 min; this time includes the time spent during

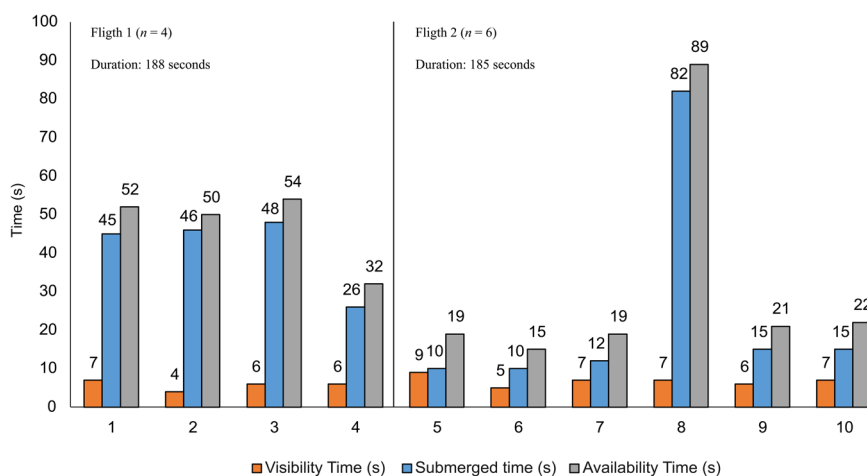


Figure 3. Bar graphs showing respiratory cycle parameters obtained from analyses of the two videos taken for the Bryde's whale. On the x-axis, values from 1 to 10 represent the respiratory cycle. The y-axis shows the time (in seconds) for each collected variable. The orange, blue, and gray colors refer to visibility, submerged, and availability time, respectively.

battery change) during the 10 observed respiratory cycles. The estimated travel speed was 1.72 m/s or 6.2 km/h.

The sighted Bryde’s whale swam at speeds like previous reports of the species (Kato & Perrin, 2018). Based on the angles of movement (approximately linear, Fig. 4) and the swimming speed, this behavior can be associated with migration or swimming. These results are consistent with those presented by Murase et al. (2016) and Liu et al. (2021) and for Bryde’s whales monitored by satellite tracking, where the linearity of the movements and continuous swimming speed observed were like those reported here and were associated with migratory behavior. In both works cited, the whales monitored presented swimming speeds slightly slower than our findings (4.4 km/h, Murase et al., 2016, and 5.33 km/h, Liu et al., 2021). Additionally, Dong et al. (2022), while monitoring Bryde’s whales in China with satellite suction transmitters, estimated an average displacement speed of 6.87 km/h during shallow water dives, a similar scenario to that reported in this study in which the whale was observed swimming at 6.2 km/h and performing shallow dives.

For the first time in Brazil, a Bryde’s whale was measured by applying aerial photogrammetry techniques. The estimated morphometric measurements provide information on numerous biological aspects of a species, such as variation in body condition (Christiansen et al., 2017, 2020; Burnett et al., 2019; Noren et al., 2019), determination of age classes (Bierlich et al., 2021; Cheney et al., 2022), assessment of swimming behavior (Irschick et al., 2021), or identification of pregnant females (Christiansen et al., 2014; Cheney et al., 2022).

Several aerial photogrammetry protocols based on scale objects proved efficient in estimating measurements in marine mammals (Christiansen et al., 2016; Burnett et al., 2019; Gray et al., 2019; de Oliveira et al, 2023). Even when it is not possible to use a precision sensor to access the flight altitude, these methods provide a simple way to measure marine mammals considering the correlation of the actual object length by their pixel length,

Table 1. The table below shows a dataset that included three measurements for each flight altitude (20, 30, 40, and 50 m) used to generate the calibration model. The table displays the calculated expected altitude (Exp Altitude) values for each flight altitude. The “Diff” column represents the difference between the Expected and observed altitude measurements. The “Object Length” column corresponds to the length of the vessel used as a scale. The “Pixel Length” column provides the pixel measurements for each analyzed image, and the “eGSD” column denotes the correction factor estimated by the ratio of Object length to Pixel length for each flight altitude.

Image Label	Altitude	Exp Altitude	Diff	Object Length (m)	Pixel Length	eGSD (m/ pixel)
20M_01.JPG	20	21.53	1.53	4.7	565.01	0.008
20M_02.JPG	20	21.38	1.38	4.7	569	0.008
20M_03.JPG	20	21.61	1.61	4.7	563.02	0.008
30M_01.JPG	30	31.61	1.61	4.7	384.83	0.012
30M_02.JPG	30	31.69	1.69	4.7	383.92	0.012
30M_03.JPG	30	31.63	1.63	4.7	384.55	0.012
40M_01.JPG	40	41.64	1.64	4.7	292.14	0.016
40M_02.JPG	40	41.45	1.45	4.7	293.48	0.016
40M_03.JPG	40	41.41	1.41	4.7	293.74	0.016
50M_01.JPG	50	52.78	2.78	4.7	230.5	0.020
50M_02.JPG	50	52.95	2.95	4.7	229.73	0.020
50M_03.JPG	50	52.69	2.69	4.7	230.88	0.020

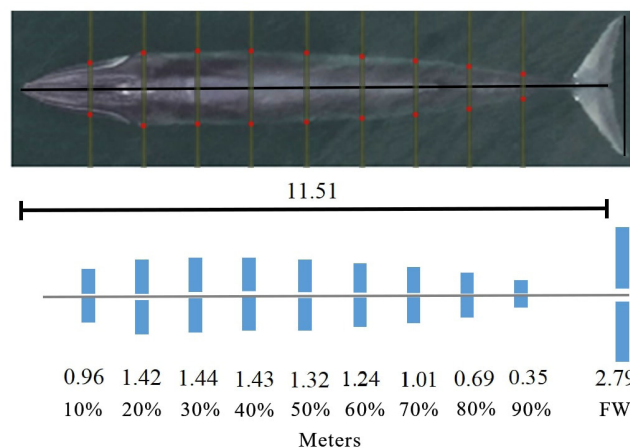


Figure 4. Bryde’s whale standardized measurements estimated. The image of the whale presented was taken at 22.3 m altitude with the DJI Phantom 4 drone. The black lines represent the total body length and the fluke width, the yellow lines represent the width (in 10% increments of total length), and the red circles delimit the outline of the body contour.

assuming a calibration model to fit the measures (Durban et al., 2016; Burnett et al., 2019).

In this work, the analysis indicates that the barometric sensor underestimates the flight altitude, as shown in Table 1, with an average error of 1.86 m. For different flight altitude classes (20, 30, 40, and 50 m), the average Exp Altitudes were 21.50, 31.64, 41.50, and 52.80 m, respectively.

The flight altitude regression model, utilized for estimating the adjustment coefficients, exhibited a coefficient of determination (r^2) value of 1. The resulting equation derived from the altitude regression model is presented below:

$$\text{Exp. Altitude} = 0.5493 + 1.0376 * \text{Altitude}$$

The fitted photogrammetric calibration model (r^2 and adjusted $r^2 = 1.00$) accurately estimated the actual length of the boat based on measurements taken at different altitudes considering the Exp Altitude as Altitude parameter. The mean length calculated by the model was 4.70 m, with a median of 4.70 m and a range of 4.69 to 4.70 m across 12 measurements (three for each altitude). The mean absolute error (MAE < 0.00) and root mean square error (RMSE < 0.00), used as model validation parameters, further confirmed the accuracy of the model in estimating boat measurements. In addition, the repeated measures collected to generate the calibration model made it possible to estimate the % Error at each flight altitude (equation 3).

$$\% \text{ Error} = | 1 - (\text{real length} / \text{estimated length}) \times 100 |$$

The percentage errors for the altitudes of 20, 30, 40, and 50 were determined to be 0.0063%, 0.0009%, 0.0034%, and 0.0051%, respectively; however, such results may be influenced by the low

Table 2. Summary of Bryde's whale measurements obtained from the applied aerial photogrammetry protocol.

Exp Altitude (m)	Body Measurement	N	Pixel Length	GSD (m/pixel)	Length (m)
22.30	Body length (BL)	2	1352	0.0082	11.13
22.30	Width at 10% of BL	2	112	0.0082	0.92
22.30	Width at 20% of BL	2	168	0.0082	1.38
22.30	Width at 30% of BL	2	170.67	0.0082	1.4
22.30	Width at 40% of BL	2	170.67	0.0082	1.4
22.30	Width at 50% of BL	2	158.67	0.0082	1.31
22.30	Width at 60% of BL	2	149.33	0.0082	1.23
22.30	Width at 70% of BL	2	120	0.0082	0.99
22.30	Width at 80% of BL	2	76	0.0082	0.63
22.30	Width at 90% of BL	2	40	0.0082	0.33
22.30	Fluke width (FW)	2	328	0.0082	2.7
32.68	Body length (BL)	2	972.44	0.0122	11.9
32.68	Width at 10% of BL	2	82.67	0.0122	1.01
32.68	Width at 20% of BL	2	119.11	0.0122	1.46
32.68	Width at 30% of BL	2	120.89	0.0122	1.48
32.68	Width at 40% of BL	2	119.11	0.0122	1.46
32.68	Width at 50% of BL	2	109.33	0.0122	1.34
32.68	Width at 60% of BL	2	102.22	0.0122	1.25
32.68	Width at 70% of BL	2	84.44	0.0122	1.03
32.68	Width at 80% of BL	2	62.22	0.0122	0.76
32.68	Width at 90% of BL	2	30.22	0.0122	0.37
32.68	Fluke width (FW)	2	236.44	0.0122	2.89

sample size (three measurements for each altitude) and by the fact that the frames were collected in only one video.

With the validation of the model, it became possible to estimate measurements for Bryde's whales by applying the equation (4).

$$\text{Estimated length} = \text{GSD} \times \text{pixel length}$$

Four frames (two at 22.30 m and two at 32.68 m of altitude, considering the Exp. Altitude) were acquired and analyzed. Bryde's whale morphometric measurements estimated for each flight altitude are shown in Table 3. The differences in the mean values calculated for each measure and altitude were not statistically significant (p -value ≥ 0.33). In this case, the standardized morphometric measurements for the Bryde's whale were considered the mean of the estimated measurements at

Table 3. Estimated standardized morphometric measurements for the Bryde's whale using the calibration model.

Body Measurement	N	Length (m)	SD (m)
Body length (BL)	4	11.51	0.38
Width at 10% of BL	4	0.96	0.04
Width at 20% of BL	4	1.42	0.04
Width at 30% of BL	4	1.44	0.04
Width at 40% of BL	4	1.43	0.03
Width at 50% of BL	4	1.32	0.01
Width at 60% of BL	4	1.24	0.01
Width at 70% of BL	4	1.01	0.02
Width at 80% of BL	4	0.69	0.06
Width at 90% of BL	4	0.35	0.02
Fluke width (FW)	4	2.79	0.09

both flight altitudes.

The estimated total body length (BL) was 11.51 m. Widths between 20% and 60% had similar values, ranging from 1.44 m (at 30%) to 1.24 m (at 60%). Above 70%, the widths gradually decrease in a proportion of approximately 30 cm to the fluke, which has a width of 2.79 m, corresponding to 24% of the body length (Table 2, Fig. 4).

Based on the morphometric measurements taken, we estimated the Fineness Ratio (FR), which represents a measure of the whale's streamline by applying the maximum body length divided by the maximum body diameter:

$$\text{Fineness Ratio} = \frac{\text{Maximum body length}}{\text{Maximum body diameter}}$$

This ratio allows us to access the hydrodynamic potential of the swimming behavior of marine mammals (Williams, 2018). The Bryde's whale FR estimated is 7.98, an expected value for rorquals such as Bryde's whales (Fish, 1993). It is considered a high FR value due to their large body length to relatively small body width. Blue whales (*Balaenoptera musculus*) show a similar high FR (6.37) to the Bryde's when compared to gray whales (*Eschrichtius robustus*) (5.64) considered an intermediary, and humpback (*Megaptera novaeangliae*) (4.21) and right whales (*Eubalaena* sp.) (4.58) that show low FR volumes (Woodward et al., 2006). The ideal FR for marine mammals is 4.5, which ensures better hydrodynamics in the marine environment, resulting in a lower drag effect (Williams, 2018).

Considering the analysis performed by the calibration model, the Bryde's whale sighted was at least 11.51 m long and presented a body width that ranged from 0.35 m (at 90% BL) to 1.44 m (at 30% BL). The body length estimated of the Bryde's whale analyzed suggests that this whale had already reached the species' mature

length, about 11.2 m for males and females (Kato & Perrin, 2018; Lima, 2020). Although the body condition assessment was not addressed in the present study, the estimated width measurements for the whale contribute to the understanding of the energy demand of the species from the variation of the body condition resulting from the ratio of body width to body length (Burnett et al., 2019; Noren et al., 2019; de Oliveira et al., 2023). However, more data from morphometric measurements of Bryde's whales are needed to obtain an effective body condition index for this species.

Regarding the aerial photogrammetry protocol, the possibility of obtaining estimates of morphometric measurements of marine mammals represents a significant methodological advance. However, it is crucial to acknowledge the inherent limitations of this approach. In the present study, various strategies were employed to address certain aspects, including the selection of appropriate frames (Burnett et al., 2019), the application of regression models to estimate the Ground Sampling Distance (GSD) correction factor (Ratsimbazafindranahaka et al., 2022; de Oliveira et al., 2023), and corrections for observed flight altitude (Burnett et al., 2019; Ratsimbazafindranahaka et al., 2022). Nevertheless, it is essential to note that certain factors, such as animal movement and the influence of climatic variables (e.g., temperature, wind speed, and sea state), have not been specifically addressed. These factors could introduce inaccuracies in determining altitude using the barometric sensor (Durban et al., 2016; Bierlich et al., 2021) and should be considered as potential sources of error in future research endeavors.

The results presented highlight the broad application of drones in monitoring marine mammals, as well as the possibility of collecting data from opportunistic encounters, especially regarding little-known species such as Bryde's whales. Information on populations of Bryde's whales found in Brazilian waters is limited and should be considered for species management. Relatively little is known regarding population size, home ranges, displacement patterns, and longevity, and the biology of these animals is poorly understood. Opportunistic sightings like this highlight the importance for researchers to collect as much data as possible to improve and advance our knowledge on the species nationally classified as Data Deficient. Finally, our results provide initial insight into the biological aspects of Bryde's whale in Brazil and urge the importance of using new technologies and interdisciplinary cetacean research and monitoring methods.

Acknowledgments

The field activities were financed by the Marine Mammal Commission (Grant number: MMC17-221), Aqualie Institute, and Grupo de Estudos de Mamíferos Aquáticos do Rio Grande do Sul - GEMARS, which provided the necessary equipment and funding for the development of this study. We are grateful for the support of Carlos Baccarin, the pilot of the boat used during collections, João Pedro Mura for his assistance during the data collection, and Joice Santos for her assistance in producing the maps.

References

- Athayde, A., Cardoso, J., Francisco, A., & Siciliano, S. (2020). Bryde's whales (*Balaenoptera brydei*) off the North Coast of Sao Paulo, Brazil: First photo-identification study. *Aquatic Mammals*, 46(5), 488–501. <https://doi.org/10.1578/AM.46.5.2020.488>
- Baxter, P. W. J., & Hamilton, G. (2018). Learning to fly: integrating spatial ecology with unmanned aerial vehicle surveys. *Ecosphere*, 9(4), e02194. <https://doi.org/10.1002/ecs2.2194>
- Bierlich, K. C., Schick, R. S., Hewitt, J., Dale, J., Goldbogen, J. A., Friedlaender, A. S., & Johnston, D. W. (2021). Bayesian approach for predicting photogrammetric uncertainty in morphometric measurements derived from drones. *Marine Ecology Progress Series*, 673, 193–210. <https://doi.org/10.3354/meps13814>
- Burnett, J. D., Lemos, L., Barlow, D., Wing, M. G., Chandler, T., & Torres, L. G. (2019). Estimating morphometric attributes of baleen whales with photogrammetry from small UASs: A case study with blue and gray whales. *Marine Mammal Science*, 35(1), 108–139. <https://doi.org/10.1111/mms.12527>
- Cheney, B. J., Dale, J., Thompson, P. M., & Quick, N. J. (2022). Spy in the sky: a method to identify pregnant small cetaceans. *Remote Sensing in Ecology and Conservation*, 1–15. <https://doi.org/10.1002/rse2.258>
- Chivers, S. J. (2009). Cetacean life history. In W. F. Perrin, B. Würsig, & J. G. M. Thewissen (Eds.), *Encyclopedia of Marine Mammals* (2nd ed., pp. 215–220). Elsevier. <https://doi.org/10.1016/B978-0-12-373553-9.00055-9>
- Christiansen, F., Dujon, A. M., Sprogis, K. R., Arnould, J. P. Y., & Bejder, L. (2016). Noninvasive unmanned aerial vehicle provides estimates of the energetic cost of reproduction in humpback whales. *Ecosphere*, 7(10), e01468. <https://doi.org/10.1002/ecs2.1468>
- Christiansen, F., Nielsen, M. L. K., Charlton, C., Bejder, L., & Madsen, P. T. (2020). Southern right whales show no behavioral response to low noise levels from a nearby unmanned aerial vehicle. *Marine Mammal Science*, 36(3), 953–963. <https://doi.org/10.1111/mms.12699>
- Christiansen, F., Sprogis, K. R., & Bejder, L. (2017, March 1-4). *Using unmanned aerial vehicles and biopsy sampling to measure body condition of humpback and minke whales in Antarctica*. Murdoch University, Australia. www.oneoceanexpeditions.com
- Christiansen, F., Víkingsson, G. A., Rasmussen, M. H., & Lusseau, D. (2014). Female body condition affects foetal growth in a capital breeding mysticete. *Functional Ecology*, 28(3), 579–588. <https://doi.org/10.1111/1365-2435.12200>
- Dawson, S. M., Hamish Bowman, M., Leunissen, E., & Sirguyev, P. (2018). Inexpensive aerial photogrammetry for studies of whales and large marine animals. *Frontiers in Marine Science*, 5, 438. <https://doi.org/10.3389/fmars.2018.00438>
- de Oliveira, L. L., Andriolo, A., Cremer, M. J., & Zerbini, A. N. (2023). Aerial photogrammetry techniques using drones to estimate morphometric measurements and body condition in South American small cetaceans. *Marine Mammal Science*, 39(3), 811–829. <https://doi.org/10.1111/mms.13011>
- Dong, L., Liu, M., Lin, W., & Li, S. (2022). First suction cup tagging on a small and coastal form Bryde's whale (*Balaenoptera edeni*)

- edeni) in China to investigate its dive profiles and foraging behaviours. *Journal of Marine Science and Engineering*, 10(10), 1422. <https://doi.org/10.3390/jmse10101422>
- Durban, J. W., Moore, M. J., Chiang, G., Hickmott, L. S., Bocconcelli, A., Howes, G., Bahamonde, P. A., Perryman, W. L., & LeRoi, D. J. (2016). Photogrammetry of blue whales with an unmanned hexacopter. *Marine Mammal Science*, 32(4), 1510–1515. <https://doi.org/10.1111/mms.12328>
- Fearnbach, H., Durban, J. W., Barrett-Lennard, L. G., Ellifrit, D. K., & Balcomb, K. C. (2020). Evaluating the power of photogrammetry for monitoring killer whale body condition. *Marine Mammal Science*, 36(1), 359–364. <https://doi.org/10.1111/mms.12642>
- Fettermann, T., Fiori, L., Bader, M., Doshi, A., Breen, D., Stockin, K. A., & Bollard, B. (2019). Behaviour reactions of bottlenose dolphins (*Tursiops truncatus*) to multirotor Unmanned Aerial Vehicles (UAVs). *Scientific Reports*, 9, 8558. <https://doi.org/10.1038/s41598-019-44976-9>
- Fettermann, T., Fiori, L., Gillman, L., Stockin, K. A., & Bollard, B. (2022). Drone surveys are more accurate than boat-based surveys of bottlenose dolphins (*Tursiops truncatus*). *Drones*, 6(4), 82. <https://doi.org/10.3390/drones6040082>
- Fish, F. E. (1993). Influence of hydrodynamic design and propulsive mode on mammalian swimming energetics. *Australian Journal of Zoology*, 42, 79–101.
- Gray, P. C., Bierlich, K. C., Mantell, S. A., Friedlaender, A. S., Goldbogen, J. A., & Johnston, D. W. (2019). Drones and convolutional neural networks facilitate automated and accurate cetacean species identification and photogrammetry. *Methods in Ecology and Evolution*, 10(9), 1490–1500. <https://doi.org/10.1111/2041-210X.13246>
- IBAMA (2002). *Portaria IBAMA No 117, 26 de dezembro de 1996*. ICMBio. https://www.icmbio.gov.br/cepsul/images/stories/legislacao/Portaria/1996/p_ibama_117_1996_protectaocetaceos_alterada_p_ibama_24_2002.pdf
- ICMBio – Instituto Chico Mendes de Conservação da Biodiversidade (2018). *Livro Vermelho da Fauna Brasileira Ameaçada de Extinção*. https://www.icmbio.gov.br/portal/images/stories/comunicacao/publicacoes/publicacoes-diversas/livro_vermelho_2018_vol1.pdf
- Irschick, D. J., Martin, J., Siebert, U., Kristensen, J. H., Madsen, P. T., & Christiansen, F. (2021). Creation of accurate 3D models of harbor porpoises (*Phocoena phocoena*) using 3D photogrammetry. *Marine Mammal Science*, 37(2), 482–491. <https://doi.org/10.1111/mms.12759>
- Júnior, J. M. D. S., Miranda, A. V. de, Attademo, F. L. N., Zanoni, S. A., & Luna, F. D. O. (2019). *Manual de boas práticas em interação com mamíferos marinhos* (1st ed.). ICMBio/CMA. https://www.icmbio.gov.br/cma/images/stories/Publica%C3%A7%C3%B5es/manual_de_boas_praticas_em_interacao_com_mamiferos_marinhos_2019.pdf
- Kato, H., & Perrin, W. F. (2018). Bryde's Whale. In B. Würsig, J. G. M. Thewissen, & K. M. Kovacs (Eds.), *Encyclopedia of Marine Mammals* (3rd ed., pp. 143–145). <https://doi.org/10.1016/b978-0-12-804327-1.00079-0>
- Lima, E. C. C. (2020). A note on strandings of Bryde's whales (*Balaenoptera edeni*) in the southwestern Atlantic. *Journal of Cetacean Research and Management*, 21(1), 9–15. <https://doi.org/10.47536/JCRM.V21I1.180>
- Liu, M., Lin, W., Lin, M., Liu, B., Dong, L., Zhang, P., Yang, Z., Wang, K., Dai, L., & Li, S. (2021). The first attempt of satellite tracking on occurrence and migration of Bryde's whale (*Balaenoptera edeni*) in the Beibu Gulf. *Journal of Marine Science and Engineering*, 9(8), 796. <https://doi.org/10.3390/jmse9080796>
- Lodi, L., & Tardin, R. (2018). Citizen science contributes to the understanding of the occurrence and distribution of cetaceans in southeastern Brazil – A case study. *Ocean & Coastal Management*, 158, 45–55. <https://doi.org/10.1016/j.ocecoaman.2018.03.029>
- Lodi, L., Tardin, R. H., Hetzel, B., Maciel, I. S. M., Figueiredo, L. D., & Simão, S. M. (2015). Bryde's whale (Cetartiodactyla: Balaenopteridae) occurrence and movements in coastal areas of southeastern Brazil. *Zoologia*, 32(2), 171–175. <https://doi.org/10.1590/S1984-46702015000200009>
- Maciel, I. S., Tardin, R. H., & Simão, S. M. (2018). Occurrence and habitat use of Bryde's whales (*Balaenoptera edeni*) in the Cabo Frio region, South-eastern Brazil. *Journal of the Marine Biological Association of the United Kingdom*, 98(5), 1081–1086. <https://doi.org/10.1017/S002531541600134X>
- Milmann, L., Siciliano, S., Morais, I., Tribulato, A. S., Machado, R., Zerbini, A. N., Baumgarten, J. E., & Ott, P. H. (2020). A review of *Balaenoptera* strandings along the east coast of South America. *Regional Studies in Marine Science*, 37, 101343. <https://doi.org/10.1016/j.risma.2020.101343>
- Murase, H., Tamura, T., Otani, S., & Nishiwaki, S. (2016). Satellite tracking of Bryde's whales *Balaenoptera edeni* in the offshore western North Pacific in summer 2006 and 2008. *Fisheries Science*, 82(1), 35–45. <https://doi.org/10.1007/s12562-015-0946-8>
- Noren, S. R., Schwarz, L., Chase, K., Aldrich, K., Oss, K. M. M. Van, & Leger, J. S. (2019). Validation of the photogrammetric method to assess body condition of an odontocete, the short-finned pilot whale *Globicephala macrorhynchus*. *Marine Ecology Progress Series*, 620, 185–200. <https://doi.org/10.3354/meps12971>
- Pastene, L. A., Acevedo, J., Siciliano, S., Sholl, T. G. C., de Moura, J. F., Ott, P. H., & Aguayo-Lobo, A. (2015). Estructura genética poblacional de la ballena de Bryde en América del Sur. *Revista de Biología Marina y Oceanografía*, 50(3), 453–464. <https://doi.org/10.4067/S0718-19572015000400005>
- Ratsimbazafindranahaka, M., Razafimahatratra, E., Mathevet, R., Adam, O., Huetz, C., Charrier, I., & Saloma, A. (2022). Morphometric study of humpback whale mother-calf pairs in the Sainte Marie channel, Madagascar, using a simple drone-based photogrammetric method. *Western Indian Ocean Journal of Marine Science*, 20(2), 95–107. <https://doi.org/10.4314/wiojms.v20i2.8>
- Thomas, P. O., Reeves, R. R., & Brownell, R. L. (2016). Status of the world's baleen whales. *Marine Mammal Science*, 32(2), 682–734. <https://doi.org/10.1111/mms.12281>
- Williams, T. M. (2018). Swimming. In B. Würsig, J. G. M. Thewissen, & K. M. Kovacs (Eds.), *Encyclopedia of Marine Mammals* (3rd ed., pp. 970–979). Elsevier. <https://doi.org/10.1016/B978-0-12-804327-1.00256-9>
- Woodward, B. L., Winn, J. P., & Fish, F. E. (2006). Morphological specializations of baleen whales associated with hydrodynamic performance and ecological niche. *Journal of Morphology*, 267(11), 1284–1294. <https://doi.org/10.1002/jmor.10474>